CLOUDS AND PRECIPITATION AT THE PHOENIX MARS LANDER SITE. C. S. Dickinson[1], L. Komguem[2] and J.A. Whiteway[3]. [1]York University, now at MacDonald Dettwiler & Associates (9445 Airport Road, Brampton, ON, CANADA, L6S 4J3, cameron.dickinson@mdacorporation.com), [2]York University (komguem@yorku.ca) [3]Centre for Research in Earth and Space Science, York University, (Toronto, ON Canada M3J 1P3, whiteway@yorku.ca)

Introduction: The Phoenix Mars mission [1] landed at 68^o N, 234^o E on 25 May 2008, 30 Martian days (Sols) before summer solstice. Over the next 5 months, the Martian atmosphere was sampled using the Meteorological or MET weather station, consisting of pressure and temperature sensors [2], as well as a lidar [3]. The vertical structure of Martian dust, as well as clouds, both within the boundary layer [4,5] and as ground fog [6], was also measured.

Over much of the 5-month mission, clouds within the Planetary Boundary Layer (PBL) of Mars were observed using the Phoenix lidar, and an analysis of their characteristics was undertaken. The focus of the present work was to determine whether precipitation plays a significant role in the seasonal cycle in atmospheric water vapor, and in particular, to what extent does water exchange between the air and ground.

Lidar Description: Vertical profiles of the atmosphere were sampled using a lidar, in which pulses of light are emitting into the atmosphere and the light scattered directly back is detected and quantified. For Mars, the lidar backscatter signal is dominated by dust and water ice cloud particles, whereas for Earth, molecular species are also observable. The Phoenix lidar is based on a Nd:YAG laser and the frequency doubled output at a wavelength of 532 nm is directed in the zenith. See Figure 1.

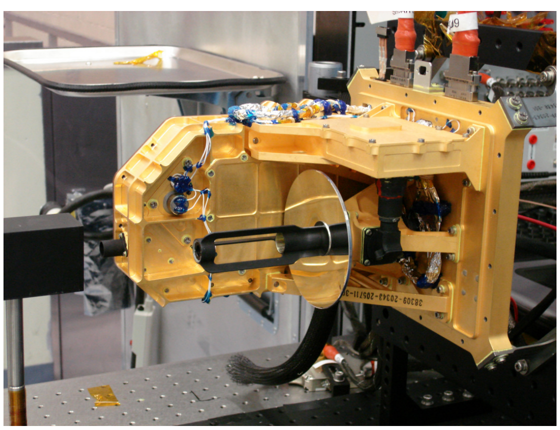

Figure 1: Phoenix Mars Lidar System

A 10 cm diameter telescope collects the backscattered light where a photomultiplier then detects it. The signal is acquired using both analog recording and photon counting, with the height resolution, after averaging, measured at 20 m and 50 m, respectively. The laser was pulsed at a rate of 100Hz, while the acquired profiles were averaged over 2048 pulses for a temporal resolution of 20.48 seconds. Typically the Phoenix lidar was operated three times per day, with total durations of between 15 minutes and one and a half hours.

Analysis: The height (z) dependant signals can be described using the Lidar equation: $S(z) = \xi(z) \times C \times \beta(z) \times 1/z^2 \times T(z)^2$. Signal reduction owing to the geometrical overlap of the laser beam and telescope field of view, $\xi(z)$, was corrected at heights below 1 km [7]. C is the calibration constant that accounts for optical throughput, detector efficiency, telescope size, and laser pulse energy. The backscatter coefficient, $\beta(z)$, is the fraction of laser pulse that is scattered back to the lidar receiver per unit length and per unit Solid angle, while the atmospheric transmission, $T(z)$, can be related to the Optical Depth (OD) as, $T(z) = e^{-OD}$, with $OD = \int_0^z \sigma dz$. These last two terms are often separated into contributions from dust and water-ice particles as $\sigma(z) = \sigma^{Dust}(z) + \sigma^{WI}(z)$ and $\beta(z) = \beta^{Dust}(z) + \beta^{WI}(z)$.

The profiles were very broadly divided into those that exhibited dust only (e.g. Sol 100: exhibiting a smooth profile of extinction coefficients up to the top of the PBL: at heights of around 4 km) and dust + cloud (e.g. Sol 95: exhibiting signal enhancements owing to the presence of clouds and ground fogs), as shown in Figure 2 [5].

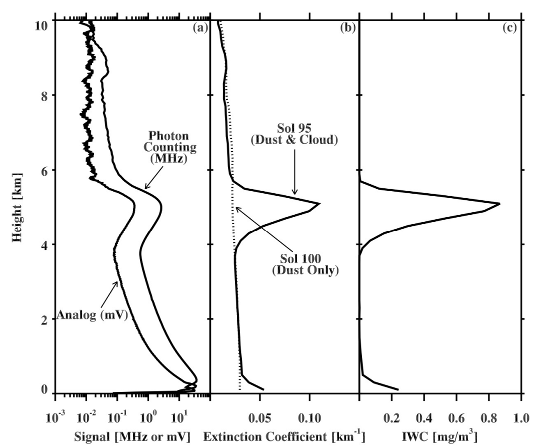

Figure 2: (a) Raw analog (mV) and photon counting (MHz) signals for Sol 95 02:45 LTST (L_S = 120) (b) Sol 100 (dust only) and Sol 95 (dust + cloud) lidar profiles (c) calculated Ice-Water content for Sol 95.

Dust extinction and backscatter coefficient profiles were derived using the method of Fernald [8] with the constraint that vertical integration of the resulting profile match the Optical Depth [9] as derived by the Phoenix Surface Stereoscopic Imager (SSI). This method requires that the ratio of extinction to backscatter coefficients ($\sigma^{Dust}/\ \beta^{Dust}$) be estimated, and a value typical of Earth Aeolian dust, 40 – as described by Papayannis [10] – was employed.

Water ice cloud extinction and backscatter coefficient profiles were also determined using the method of Fernald [8], but instead employed the daytime dust-only profiles as a reference, rather than constraining the integrated profile to values of optical depth. Here a value of extinction to backscatter coefficients ($\sigma^{Dust}/\ \beta^{Dust}$) for ice was estimated to be 15 – typical of Earth cirus clouds [11]. Ice-Water Content (*IWC*) was then derived from the extinction coefficient, employing the empirical relationship of $IWC = 10.0\sigma^{IW}$ as determined by Dickinson [12], while the Column IWC was calculated as $IWC_{Column} = \int_0^z IWC\ dz$, or simply ten times the Ice-Water Optical Depth.

Results: As reported by Dickinson [5], a repeating diurnal pattern of water-ice cloud formation was observed between Sols 80 (L_S = 113) and Sol 128 (L_S = 137), as shown in Fig. 3.

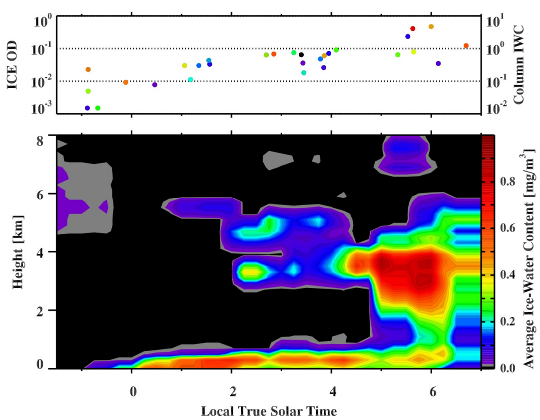

Figure 3: Contour plot of average IWC as a function of Local Solar Time between Sols 80 and 148 (L_S = 113 to 147) shown at bottom and the integrated Water-Ice optical depth, and resulting Column IWC is given above.

Ground level ice-fogs were observed to onset at around 23:00, with clouds at or near the top of the PBL forming at around 01:00. Over the next four to five hours the cloud base was observed to descend, often filling the entire PBL with water-ice clouds. Following 07:00, the air temperature within the PBL increased with Solar heating, causing the water-ice clouds to dissipate. The column IWC for each individual profile is also given in Fig. 3, increasing throughout the night and reaching a maximum at approximately 06:00.

Conclusions: The frost point of the air decreased with time, owing to cloud formation not beng observed earlier than 01:00, and as the season progressed the air temperature decreased. The air temperature at height 4 km was calculated from a numerical model of the PBL of Mars [4]. It was estimated that between mission Sols 95 and 145 (L_S 120 to 145) that the temperature decreased from –64.3 °C to –70.2 °C, equating to saturated water vapor densities of 6.8 and 2.9 mg/m^3, respectively. Assuming a well mixed PBL from ground to a height of 4 km, the total PBL water column decreased from 33 and 14 g/m^2, or 19 g/m^2, over this period. A similar decrease was observed by the CRISM instrument, on board the Mars Reconnaissance Orbiter (MRO), which observed the total water column above the Phoenix landing site to decrease from 44 g/m^2 to 22 g/m^2 between Sols 99 and 150 [8]. This analysis indicates that the seasonal cycle in atmospheric water vapor occurs mainly within the PBL. The extent to which the water vapor interacts with the ground, and the amount of water vapout above the PBL, would be required for a complete picture of the local water cycle, and are the subject of future work.

References: [1] Smith, P. H. et al., (2009) *Science 325*, 58-61. [2] Taylor, P. et al., (2009) *J. Geophys. Res. - Planets 113*, E00A10. [3] Whiteway, J. et al. (2008) *J. Geophys. Res. - Planets 113*, E00A08. [4] Whiteway, J. et al., (2009) *Science, 325,* 68-70. [5] Dickinson, C. S. et al. (2010) *GRL, 37,* L18203, 5 PP. [6] Moores, J. E. et al. (2010) *GRL, 38*, L04203. [7] Whiteway, J. A. and Dickinson, C. S. (2010) *NASA Planetary Data System – Planetary Atmospheres Node.* [8] Fernald, F. G. (1984) *Applied Optics*, *23(5),* 652-653. [9] Tamparri, L. K. et al. (2009) *J. Geophys. Res. – Planets, 115*, E00E17, 25 PP. [10] Papayannis et al. (2008) *J. Geophys. Res.*, 113, 2000–2002. [11] Chen, W-N. et al. (2002) *Applied Optics,* 41, 6470–6476. [12] Dickinson, C. S. et al (2010) *Planetary Space Science 59(10),* 942-951.